Journal of Membrane Science 679 (2023) 121710

Contents lists available at ScienceDirect

Journal of Membrane Science

journal homepage: www.elsevier.com/locate/memsci

Nanoporous thin films of hydrophobic block copolymers enabled by selective swelling for membrane distillation

Zhuo Li, Shoutian Qiu **, Xiang Ying, Fangli Zhang, Xianli Xu, Zhaoliang Cui, Yong Wang *

State Key Laboratory of Materials-Oriented Chemical Engineering, College of Chemical Engineering, Nanjing Tech University, Nanjing, 211816, Jiangsu, PR China

ARTICLE INFO

Keywords:
Membrane distillation (MD)
Block copolymer
Selective swelling
Polydimethylsiloxane (PDMS)
Liquid entry pressure (LEP)

ABSTRACT

Membrane distillation (MD) is receiving growing interest because of its >99.9% salt rejection even with low-grade waste heat as the energy supply. However, MD membranes are prone to be wetted and usually require complicated modification strategies to gain sufficient hydrophobicity. In this work, we report a new type of MD membranes with hydrophobic films carrying pores in the ultrafiltration range as the separation layers. Such membranes are prepared by coating an A-B-A triblock copolymer polystyrene-*block*-polydimethylsiloxane-*block*-polystyrene (PS-*b*-PDMS-*b*-PS, further abbreviated as SDS) on the macroporous PVDF substrate, followed by soaking in alkanes to cavitate the SDS coating layers following the mechanism of selective swelling. The PDMS microdomains in the SDS layers are converted to interconnected nanopores, and the PDMS blocks are enriched along the pore walls and membrane surface, endowing the membranes with intrinsic hydrophobicity. Thus-prepared SDS membranes exhibit stable rejection to NaCl (>99.99%) and high permeate flux up to 32.8 kg m^{-2} h^{-1}, better than most MD membranes with large pores in the microfiltration range. Moreover, the SDS membranes display excellent wetting resistance, good heat resistance, and long-term stability. This work provides a new strategy to prepare MD membranes enabled by selective swelling of hydrophobic block copolymers, and demonstrates the great potential of hydrophobic ultrafiltration membranes in the long-term use in membrane distillation.

1. Introduction

Membrane distillation (MD) has attracted growing attentions because of its capability to achieve larger than 99.9% salt rejection with relatively low cost utilizing low-grade waste heat sources as the energy supply [1–4]. The process of MD uses hydrophobic membranes with interconnected pores as a liquid barrier, which only allows vapors to pass through while the liquid feed including dissolved components is retained under heating conditions, thus separating the vapor phase from the liquid phase within the membrane pores [5–7]. To date, MD has shown potential applications in many fields including desalination of seawater [8], juice concentration [9], alcohol fermentation [10], and removal of chemical volatile substances [11]. Typically, MD has been proven to be a more effective and energy-efficient process to desalinate seawater and brines compared with conventional desalination methods such as multi-stage flash [3,8].

Membranes with a hydrophobic surface and porous structure are of ultimate importance in MD processes [5,12,13]. Usually, hydrophobic membranes used in MD are mainly prepared by polyvinylidene fluoride (PVDF) [14], polytetrafluoroethylene (PTFE) [15], polyethylene (PE) [16] and polypropylene (PP) [17], etc. These membranes are typical commercial microfiltration membranes, *i.e.* with pore sizes among ~0.1–1 μm, and exhibit moderate surface hydrophobicity [2,3]. However, the moderate surface hydrophobicity and large pore size of these membranes usually result in a relatively low liquid entry pressure (LEP) [18], which allows liquid water enters the membrane pores at low pressures or causes solute enrichment on membrane surface, thus hindering the long-term performance in MD [19]. Constructing superhydrophobic membrane surfaces has been recently demonstrated to be one of the most effective strategies to prevent membrane wetting on account of their extremely high water contact angles (WCAs) [13]. Recent studies regarding the preparation of superhydrophobic membranes mostly rely on increasing the surface roughness and lowing the surface energy of the membrane-forming materials [2], including surface chemical modification [20,21], plasma treatment [22], as well as the utilization of nanoparticles and polymers with low surface energy

* Corresponding author.
** Corresponding author.
E-mail addresses: qiust@njtech.edu.cn (S. Qiu), yongwang@njtech.edu.cn (Y. Wang).

https://doi.org/10.1016/j.memsci.2023.121710
Received 3 April 2023; Received in revised form 24 April 2023; Accepted 30 April 2023
Available online 6 May 2023

[23,24]. However, these methods are usually suffering from tedious processes, expensive modifying agents, and copious consumption of organic solvents. Therefore, it is highly demanded to develop facile but efficient strategies to prepare MD membranes with long-standing desalination performances.

The hydrophobicity, pore size, porosity and effective film thickness play key roles in determining the performance of MD [7,25,26]. According to the Young-Laplace's equation [27], improving the hydrophobicity (*i.e.* WCA) is not the only way to promote the LEP of membranes, and lowering the pore size is also able to increase the wetting resistance (*i.e.* LEP) of membranes. Typically, liquid water is more difficult to enter pores with smaller sizes, leading to higher LEPs and consequently better wetting resistance. Therefore, membranes with smaller pore size tend to tolerate surface wetting even with relatively low hydrophobicity [28,29]. However, smaller pore sizes may result in narrowed transfer channels, leading to lower permeate flux [25]. Currently, there is a lack of studies on the effect of pore size on the MD performance. Few ultrafiltration membranes and nanofiltration membranes with hydrophobic surfaces have been used for the MD purpose [30,31], and it is highly demanded to investigate the possibility of ultrafiltration and nanofiltration membranes in MD. In this paper, we coat thin hydrophobic layers with pore sizes in the ultrafiltration range onto the macroporous substrates to prepare a new type of MD membranes with long-standing wetting resistance and excellent MD performance.

Very recently, we reported a facile and nondestructive strategy of preparing hydrophobic membranes with nanoporosities using selective swelling of hydrophobic block copolymers (BCPs) [32]. High porosity is achieved by soaking polystyrene-*block*-polydimethylsiloxane-*block*-polystyrene (PS-*b*-PDMS-*b*-PS, abbreviated as SDS below) dense films in alkanes at room temperature. As-prepared hydrophobic porous films are penetrated with interconnected pores of tens of nanometers falling in the ultrafiltration range and display inherent surface hydrophobicity thanks to the enrichment of the more hydrophobic PDMS blocks onto the membrane surface as well as pore walls. Such an intrinsic hydrophobicity and interconnected nanoscale porosity imply that thus-prepared SDS membranes may show new possibility and potential in MD. Besides, PDMS has been utilized in the coating modification of MD membranes owing to the low surface energy and intrinsic hydrophobicity; however, crosslinking is inevitable on account of the rubber state and fluidity of PDMS at room temperature [33,34]. Interestingly, the PS phase in SDS functioned as physical crosslinking points to prevent PDMS chains from flowing discretionarily, therefore, the SDS BCPs were not needed to be further crosslinked and could be repeatedly used. In this paper, we report the preparation of composite MD membranes with hydrophobic nanoporous SDS coatings enabled by selective swelling as the function layers, and demonstrate the feasibility and distinguished performances of hydrophobic membranes with pores in the ultrafiltration range as a strong player for MD. Besides, the effect of pore size, porosity and effective film thickness on membrane distillation performance are systematically investigated.

2. Experimental section

2.1. Materials

Styrene (≥99.9%), bis(aminopropyl)-functionalized PDMS (with M_n of PDMS ~5, 10, and 25 kDa, respectively), 4,4'-azobis (4-cyanovaleric acid) (ACVA, ≥98.0%), dicyclohexylcarbodiimide (DCC, ≥98.0%), and N, N-dimethylpyridin-4-amine 4-methybenzenesulfonate (DPTS, ≥98.0%) were provided by Energy Chemical. *n*-hexane (C6, ≥95%) was purchased from Sigma Aldrich. N, N-dimethylformamide (DMF, ≥99.9%) and *n*-octane (abbreviated as C8, ≥95%) were supplied by Macklin. *n*-heptane (abbreviated as C7, ≥99.0%), anhydrous tetrahydrofuran (≥99.9%), *n*-decane (abbreviated as C10, ≥99.0%) and sodium dodecyl sulfate (≥99.0%) were obtained from Aladdin. Anhydrous ethanol (≥99.8%), chloroform (≥99.0%), methanol (≥99.7%) and NaCl (≥99.8%) were purchased from local suppliers. Silicon wafers were treated by ultrasonic cleaning before using. Hydrophilic PVDF membranes with the nominal pore size of 0.22 μm were purchased from Millipore and used as macroporous substrates to prepare composite membranes. All reagents were used as received. Deionized water (DI water) with a conductivity of 8–20 μS cm^{-1} was used in all tests.

2.2. Synthesis of SDS BCPs

SDS BCPs with varied PDMS contents and molecular weights were synthesized from the PDMS macroinitiators and styrene monomer following our previous work [34]. First, we used bis(aminopropyl)-functionalized PDMS to synthesize PDMS macroinitiators at room temperature for 48 h. Then, a preset amount of PDMS macroinitiator, styrene, as well as the solvent, anhydrous tetrahydrofuran, were added into a reaction flask followed by degassing and sealing under vacuum. The polymerization of styrene was initiated by the PDMS macroinitiators, and the reaction took place at 80 °C for 24 h. After purification, as-synthesized SDS copolymers with the molecular weight of the PDMS block of 5k, 10k, and 25k were named as SDS5k-X, SDS10k-X, and SDS25k-X, respectively, in which X represents the weight percentage value calculated by ^{1}H NMR. For example, SDS10k with 21.5 wt% PDMS was denoted as SDS10k-22.

2.3. Selective swelling of SDS thin films

The casting SDS solution with a concentration of 2 wt% in chloroform was repeatedly filtrated through 0.22 μm PTFE filters three times before use. To investigate the swelling behavior of SDS BCPs with different contents, the dense BCP films were fabricated by spin-coating BCP solutions onto silicon wafers at 2000 rpm for 30 s (Fig. S1). The obtained films were then soaked in alkanes with varied carbon numbers (C6, C7, C8, C10) at 25 °C for 1 h to perform selective swelling. After swelling, the films were taken out from the solvent and dried at ambient conditions for at least 24 h to evaporate the volatile alkanes.

2.4. Preparation of SDS composite membranes

Hydrophobic SDS composite membranes were prepared by coating SDS solutions onto macroporous PVDF substrates (Fig. S1). Before coating, hydrophilic PVDF substrates which have a WCA of 0° (Fig. S2) were immersed in DI water for 30 min to fill the pores with water to avoid the leakage of SDS solutions during the coating process. After being removed from water, the PVDF substrates were placed on a clean glass plate. SDS solutions were spin-coated on PVDF substrates (2000 rpm, 30s), followed by drying at 25 °C for at least 24 h. Afterwards, the SDS-coated PVDF substrates were soaked in alkanes at 25 °C to perform selective swelling to the SDS layers. After certain durations, the samples were removed from alkanes, and dried at ambient conditions for at least 24 h, thus obtaining composite membranes with hydrophobic nanoporous SDS coating layers (Fig. 1). The WCAs of the composite membranes were ~120° (Fig. S3).

2.5. Characterizations

The chemical structures of synthesized SDS BCPs were determined by ^{1}H nuclear magnetic resonance (^{1}H NMR, AV400, Bruker) using $CDCl_3$ as the solvent. Thermogravimetric analysis (TGA) was conducted using a synchronous thermal analyzer instrument (Netzsch, STA 449 F3). The TGA curves from room temperature to 800 °C were recorded at 10 °C·min^{-1} under N_2. The cross-sectional and surface morphologies were recorded using a Hitachi S-4800 field emission scanning electron microscope (FESEM) under an accelerating voltage of 3 kV. Before testing, the SDS films were sputter-coated with platinum to increase the electrical conductivity. Besides, the samples used for cross-sectional observation were immersed in liquid nitrogen and ruptured.

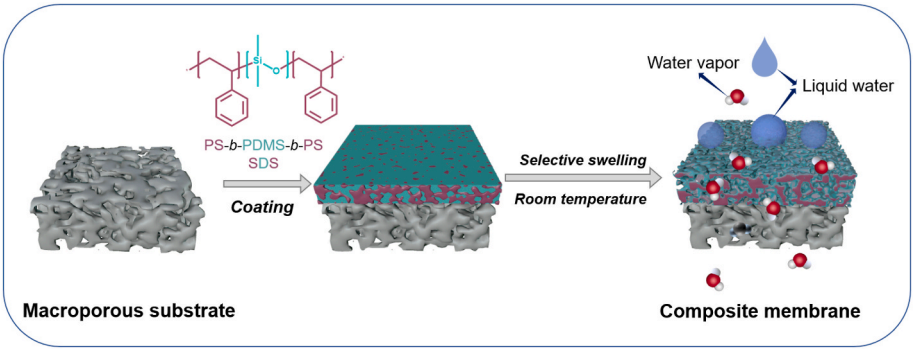

Fig. 1. Schematic diagram of the preparation of SDS composite membranes via coating and selective swelling.

The thicknesses of SDS films coated on the silicon wafer before and after swelling were tested via a spectroscopic ellipsometer (Complete EASE M − 2000U, J. A. Woollam) with an incidence angle of 70°. The volume porosities of the SDS films were then calculated by comparing the film thickness before and after swelling. The surface porosities, however, were estimated by measuring the proportion of pore area on the film surface from SEM images.

2.6. Wetting resistance tests

Wetting resistance of MD membranes is generally characterized by LEP. LEP is the maximum pressure value that liquid cannot pass through the membrane pores. The LEP value can be calculated by the Young-Laplace's equation.

$$LEP = \frac{-2B\gamma_l \cos\theta}{r_{max}} \quad (1)$$

where r_{max} is the maximum pore size of surface pores on SDS coating layers after swelling. γ_l represents the liquid surface tension while θ is the water contact angle. B is a geometric factor involving pore morphologies [27,35]. In this work, a dynamic measurement technique was applied on a cross-flow filtration device to determine the practical LEP experimentally. The SDS composite membrane was put into the cross-flow filtration device where deionized water was recirculated at 20 °C. Then the hydrostatic pressure on the feed side is increased from 0.1 to 6 bar by a step of 0.1 bar every 5 min. The LEP value was determined as the pressure at which the first drop of liquid water was observed. Each measurement was carried out three times, and the average value and standard deviation were reported.

2.7. Membrane distillation tests

The MD of SDS composite membranes was operated on a homemade apparatus with an effective membrane area of 1.19 cm^2 utilizing the vacuum membrane distillation (VMD) process (Fig. S4). During the VMD test, the hydrophobic SDS side was facing the feeding NaCl solution while the PVDF side supported by a steel mesh was facing the vacuum. The membranes used in MD tests were prepared by selective swelling in C6 at 25 °C. The operating temperature was controlled at 50 °C by a water bath and the flow rate of feed solution (a 0.6 M NaCl aqueous solution) was fixed at 500 mL min^{-1} using a peristaltic pump. The temperature of the condensation water was set as 1 °C while the pressure was kept at 2 kPa on the permeate side. The MD test was first stabilized for 2 h, and then lasted for 8 h. The mass and conductivity of the distillate (permeate solution) were measured every 1 h via an electronic balance and a conductivity meter (S230–K, Mettler Toledo), respectively. The permeate flux (J) was calculated using Eq. (2)

$$J = \frac{W}{A \cdot t} \quad (2)$$

where J ($kg \cdot m^{-2} \cdot h^{-1}$) is the permeate flux, W (kg) is the mass of distillate. A (m^2) and t (h) are the effective membrane area and the recording time, respectively. The salt rejection of membrane (R, %) was computed via Eq. (3)

$$R = \left(1 - \frac{\mu_p}{\mu_f}\right) \times 100\% \quad (3)$$

where μ_p ($\mu S \cdot cm^{-1}$) and μ_f ($\mu S \cdot cm^{-1}$) represent the conductivity of the permeate solution and the feed solution, respectively.

The long-term MD performance was conducted on the SDS10k-22 membrane. The test was run continuously for 156 h with a 0.6 M NaCl feeding solution. The feed temperature was set at 50 °C, and the permeated liquid was returned to avoid the variation of the feed solution concentrations. A 0.6 M NaCl aqueous solution containing 0.05 mM sodium dodecyl sulfonic acid was also used to test the effect of surfactants on the long-term MD performance of the SDS10k-22 membrane. Besides, the MD performances were tested at different heating temperatures ranging from 30 to 80 °C to evaluate the heat resisting property of the SDS composite membranes.

3. Results and discussion

3.1. Synthesis of SDS block copolymers

Several SDS BCPs with varied PDMS contents were synthesized. The block ratios were examined with ^{1}H NMR and TGA, and the results are illustrated in Fig. 2 and Table 1. As shown in Fig. 2a, all three SDS10k BCPs exhibited two-step degradation curves, in which PS segments degraded at the temperature region of 300–360 °C while the PDMS blocks degraded after 360 °C, implying that BCPs with varied PDMS contents were successfully synthesized. The block ratios of PDMS could be estimated from the degradation curves to be 11.7 wt%, 20.5 wt%, and 28.7 wt%, respectively. Meanwhile, the percentage of PDMS can also be determined according to the proton signals of PS (6.5 ppm and 7.0 ppm) and PDMS (0.08 ppm) from ^{1}H NMR spectra. The weight percentages calculated by ^{1}H NMR were 11.8, 21.5 and 30.2% for the three BCPs, respectively, which were very close to the feed ratios of the two blocks. Besides, the results in ^{1}H NMR were also close to those obtained from TGA. Given that NMR is a more accurate technique to analyze the composition of BCPs, the weight percentages calculated by ^{1}H NMR were considered as the real values and used in this work. These synthesized SDS BCPs were named as SDS10k-12, SDS10k-22, and SDS10k-30, respectively. Furthermore, to investigate the effect of chain length (the molecular weight of the PDMS block) on the swelling behavior and pore sizes, we also synthesized SDS5k-24 and SDS25k-20 following the same procedure, and the corresponding compositions were also displayed in Table 1 and Fig. S5.

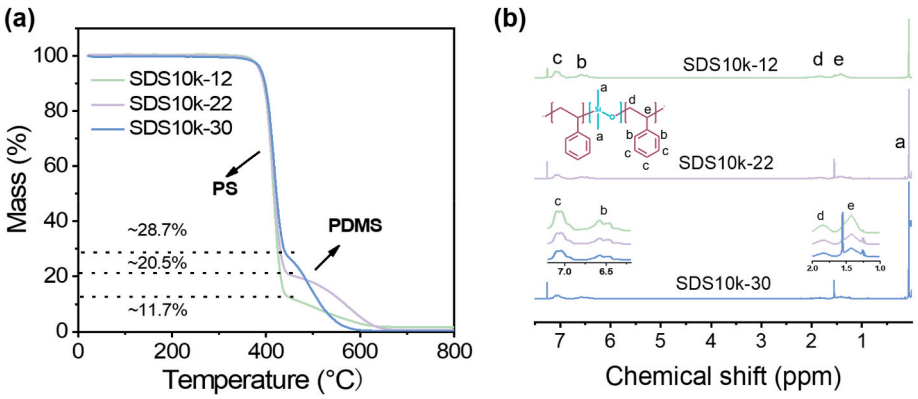

Fig. 2. (a) TGA curves and (b) ^{1}H NMR spectra of SDS10k-12, SDS10k-22, and SDS10k-30.

Table 1
The feed percentage, and weight percentage of PDMS calculated by ^{1}H NMR and TGA of SDS BCPs.

Samples	Feed percentage (%)	Weight percentage calculated by ^{1}H NMR (%)	Weight percentage calculated by TGA(%)
SDS10k-12	10	11.8	11.7
SDS10k-22	20	21.5	20.5
SDS10k-30	30	30.2	28.7
SDS5k-24	20	23.8	NA
SDS25k-20	20	20.1	NA

3.2. Effect of PDMS contents

According to our previous work, alkanes can produce well-defined nanoporosities in hydrophobic SDS films following the principle of selective swelling [32]. When soaked in alkanes, the PDMS microdomains dispersed in the PS matrix are strongly swollen, forming a new continuous phase thanks to the strong interaction between alkanes and the PDMS blocks. With the evaporation of alkanes, the swelling PDMS phases collapse, leading to interconnected pores with the PDMS chains lined along the pore walls and the film surface. This endows the SDS membrane with an intrinsic hydrophobic surface. Thus-produced porous films could achieve a volume porosity as high as 50% by simply soaking SDS10k-15 in C8, however, an elevated temperature (e. g. 55 °C) was required. However, swelling at room temperature is more desired in real-world applications for the sake of lower energy consumption and environmental risks [36]. Unfortunately, swelling SDS10k-15 films at room temperature could produce a volume porosity of no more than 42% [32]. Considering that the volume porosity is also greatly influenced by the block ratio of BCPs [37,38], we believe that SDS with sufficiently high content of PDMS can achieve considerably high volume porosity when swelling-treated at room temperature.

Three SDS BCPs (SDS10k-12, SDS10k-22, and SDS10K-30) were coated onto silicon wafers, and soaked in alkanes for 1 h to determine the appropriate PDMS percentage reaching the strongest swelling degrees (i.e. the highest volume porosity) at 25 °C. The changes in volume porosities and surface SEM images of the SDS films with varied PDMS percentages and the carbon number of alkanes after swelling are displayed in Fig. 3 and Fig. S6. As shown in Fig. 3a, the volume porosities of swollen SDS films depended not only on the kind of selective solvents but also on the composition of BCPs. SDS-10k-12 and SDS10k-22 both exhibited gradually declined swelling degrees with the increasing carbon numbers of alkanes as a result of smaller interactions between

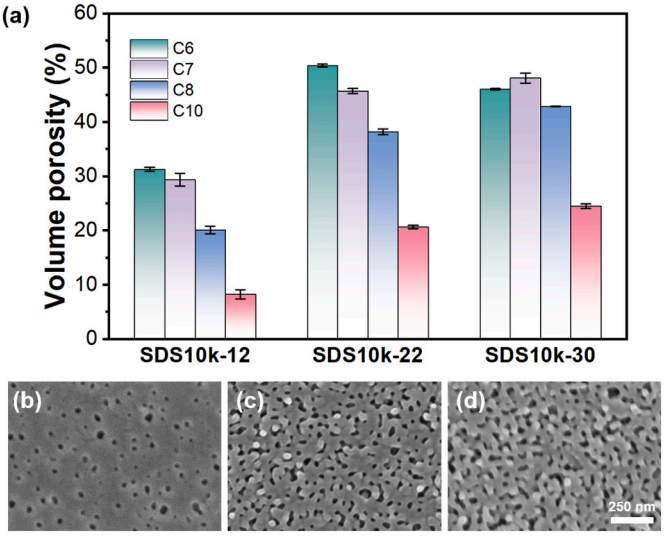

Fig. 3. (a) Evolution of volume porosities with varied PDMS contents after swelling at 25 °C in different alkanes for 1 h. Surface SEM images of (b) SDS10k-12, (c) SDS10k-22, and (d) SDS10k-30 films after swelling in C6 at 25 °C for 1 h. All images have the same magnification as the scale bar given in (d).

alkanes and BCPs [32]. However, when the PDMS percentage was increased to 30 wt%, volume porosities of the membranes soaked in C6, C7, C8 and C10 were 46.0%, 48.0%, 42.9% and 24.4%, respectively. Interestingly, the volume porosity of the SDS10k-30 film soaked in C6 was even lower than that soaked in C7. As the molecular weight of PDMS is invariable for SDS10k copolymers, the chain length of PS decreased for SDS10k with larger PDMS percentages. SDS10k-30 has the shortest PS chains, which is easier to move under pressures gradually accumulated by the expansion of PDMS. Therefore, the excessive swelling of the SDS with the highest percentage of PDMS was found in C6 because C6 has the strongest affinity to PDMS among the four alkanes [32,37]. It is clear that the volume porosity was increased evidently with the increase of the PDMS percentage except for the cases using C6 as the swelling agent. Moreover, SDS10k-22 exhibited the highest volume porosity of 50.2% when swelling was performed in C6 at 25 °C, which is comparable to the highest value obtained by SDS10k-15 (C8, 55 °C). This is almost the highest porosity value ever achieved in the selective swelling process, and it is significant when considered that it is achieved at room temperature.

The surface morphologies of the nanoporous films obtained by swelling in C6 for 1 h are displayed in Fig. 3b–d. For SDS10k-12, the surface porosity was as low as 2.9% with sparse circular lying on the film

surface, and the average pore size was just 19.9 nm. For SDS10k-22 with the PDMS percentage increased to 22%, a typical bicontinuous structure with interconnected pores was observed, and the surface porosity and pore size rose to 14.7% and 24.3 nm, respectively. For SDS10k-30, the film surface became slightly micellization as a result of a stronger swelling degree, and the surface porosity and pore size were decreased to 11.6% and 22.6 nm, respectively. Besides, as shown in Fig. S6, when swelling in C7, C8, and C10, the surface porosity and pore sizes could be enhanced with increased PDMS percentage and decreased carbon numbers in alkanes. Conclusively, SDS10k-22 films achieved the highest volume porosity and surface porosity when swelling at room temperature. Therefore, 22% was adopted as the most suitable PDMS percentage and was utilized in our following investigations.

High hydrophobicity and good wetting resistance are crucial for MD membranes. The hydrophobicities of PVDF substrates and SDS composite membranes were examined by dripping water directly on the membrane surface. As is shown in Fig. 4a, colored water was unable to wick through the membrane thanks to the hydrophobicity of the coated SDS layer while the 0.22 μm macroporous PVDF substrate was easily wetted by liquid water, verifying that the porous thin layer of SDS10k-22 endowed the substrate with strong hydrophobicity. As displayed in Fig. 4b, the PVDF substrate exhibited an irregular macroporous surface structure, the practical pore size is determined to be 280 ± 38 nm (ImageJ). Besides, the dynamic contact angle of PVDF substrate was shown in Fig. S2. Liquid water passes through the hydrophilic PVDF within 5 s. After coating of the SDS layer followed by selective swelling, the PVDF substrate was covered with a uniform nanoporous layer with a surface WCA of ~120°.The thickness of the coating layer was ~650 nm while the pore size was dozens of nanometers (Fig. 4c and d). The improvement of hydrophobicity and reduction of pore size were also beneficial in improving the wetting resistance during the MD process.

The MD performance of the SDS10k-22 membrane subjected to swelling in C6 (25 °C, 1 h) was tested and shown in Fig. 4e. The membrane showed consistent and relatively stable permeate flux (the mean permeate flux was 13.8 kg m^{-2} h^{-1}) and maintained a salt rejection above 99.99% during an 8-h test duration. Therefore, we have demonstrated that SDS films could form interconnected pores by a simple yet effective selective swelling process even at room temperature, and thus-obtained composite membranes showed great potential in the applications of MD.

3.3. Effect of PDMS molecular weights

Considering the porosities and pore sizes of the nanoporous films after selective swelling are also affected by the molecular weight of the minority blocks, we also investigated the effect of the PDMS molecular weights on the SDS film morphologies and MD performances. We investigated the swelling behaviors of SDS films with the PDMS percentage fixed at ~20–24% but the PDMS molecular weights varied among 5k, 10k, and 25k. As shown in Fig. 5a, all three samples achieved rather high volume porosities after swelling at C6 for only 1 min, and reached the equilibrium swelling condition within 1h. Afterwards, the volume porosities changed little even with an extended swelling time of 4 h. Therefore, the change of the volume porosity has little relation to the molecular weight of PDMS but is strongly affected by its contents in the copolymer.

However, the morphology of surface pores changed greatly with the PDMS molecular weight as shown in Fig. 5b–d. For SDS10k-22, most of the surface pores were between 10 and 40 nm, and the average pore size was ~24 nm. SDS5k-24 with a shorter chain length of PDMS displayed a narrower pore distribution while the surface pores were between 10–20 nm, and the average pore size was only ~14 nm. When the molecular weight of PDMS was increased to 25 kDa, the film surface showed large and sparse pores with a mean diameter of ~41 nm. Therefore, we understand that the molecular weight of PDMS greatly influenced the pore size during selective swelling. The surface pore sizes were increased significantly with the molecular weight of PDMS as a result of the increased size of the PDMS microdomains in the original SDS films before swelling for the SDS with longer PDMS blocks. Besides, the surface porosities of SDS films for SDS5k-24, SDS10k-22 and SDS25k-20 were 11.2%, 14.7%, and 9.2%, respectively, which were only varied slightly regardless of their discrepancy in the molecular weight of PDMS (Fig. 6a). Therefore, increasing the molecular weight can only effectively enlarges the pore size of the swelling-treated films, but hardly influences their porosities.

We tested the MD performance of the three SDS membranes. The permeate flux of the SDS5k-24, SDS10k-22, and SDS25k-20 membranes were 13.8, 13.2, and 13.2 kg m^{-2} h^{-1}, respectively, and they all

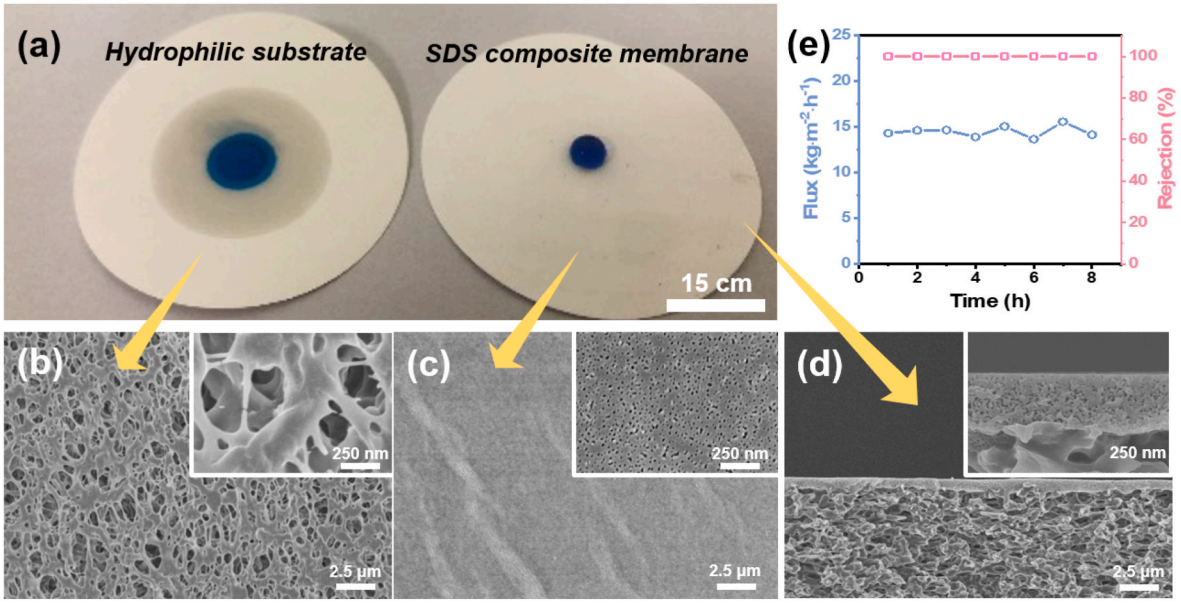

Fig. 4. (a) Digital photographs of microporous PVDF substrates (left) and the SDS10k-22 membrane (right) exposed to water drops. Surface SEM image of (b) the PVDF substrate and (c) the SDS10k-22 membrane. (d) Cross-sectional SEM image and (e) MD performance of the SDS10k-22 membrane. The SDS10k-22 membrane was prepared by swelling in C6 for 1 h. Insets in (b–d) show the corresponding magnified SEM images.

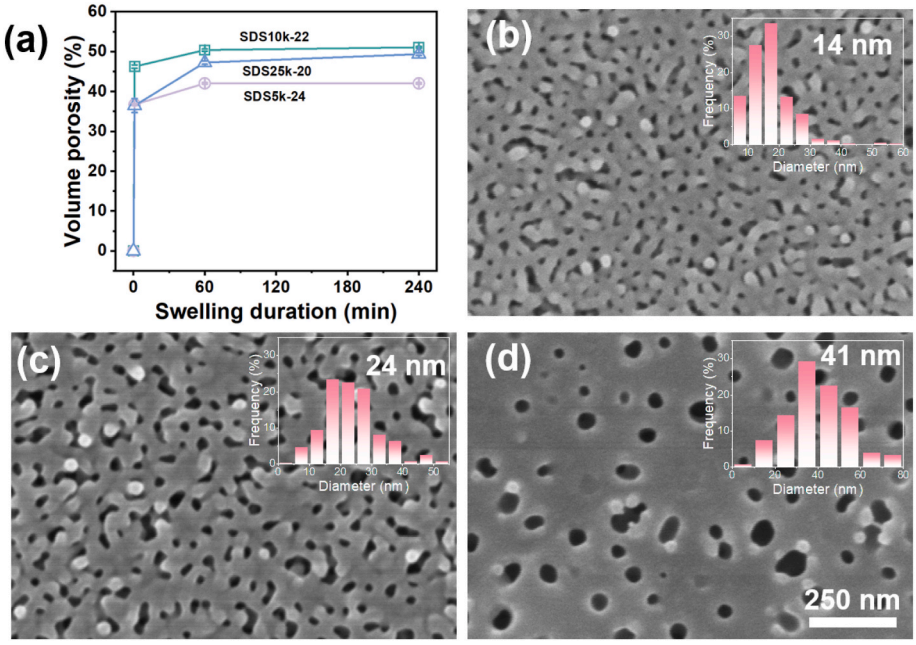

Fig. 5. (a) Variations of volume porosities of SDS films with different molecular weights of PDMS after swelling in C6 at 25 °C. Surface SEM images of (b) SDS5k-24, (c) SDS10k-22, (d) SDS25k-20 films after swelling in C6 (25 °C, 1 h). All images have the same magnification as the scale bar given in (d). Insets in (b–d) show the pore size distribution and the average pore size of the corresponding membranes.

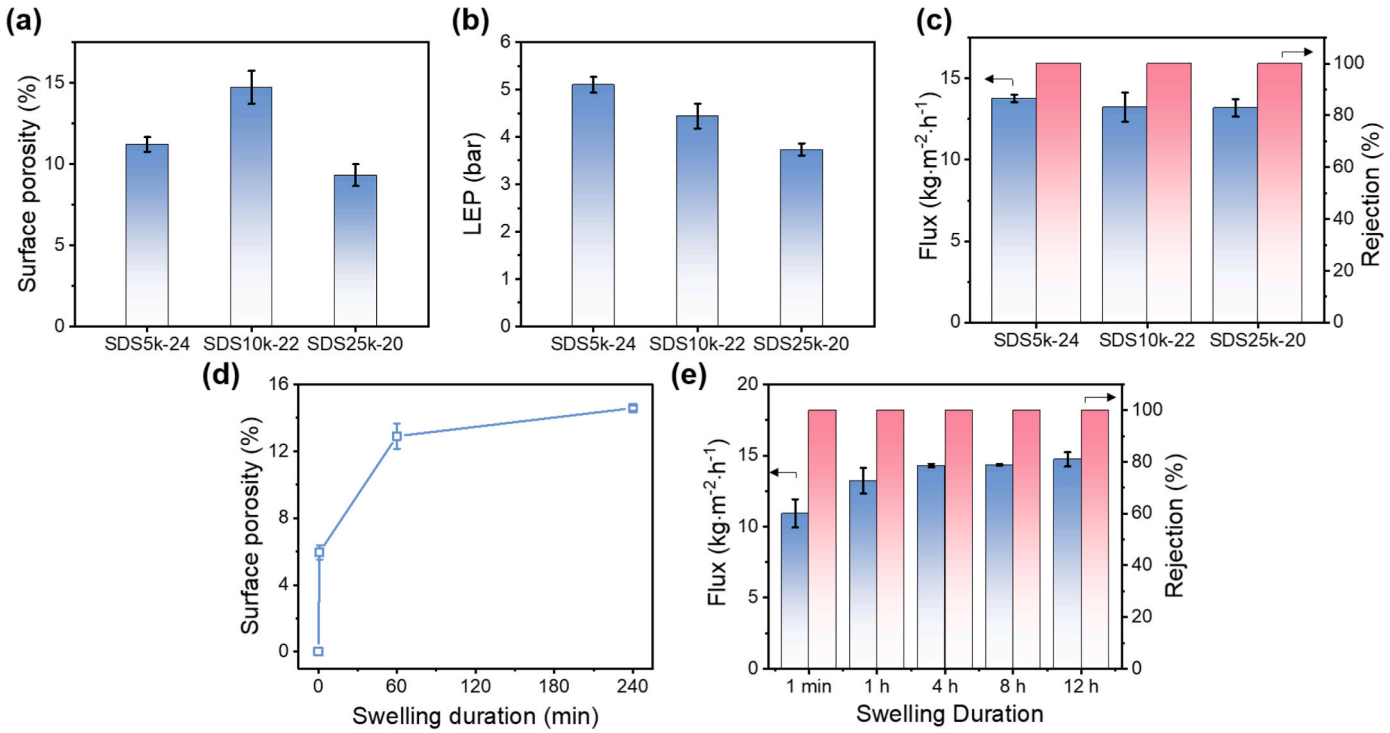

Fig. 6. (a) Surface porosities, (b) LEP values, and (c) MD performance of the SDS5k-24, SDS10k-22, and SDS25k-20 composite membranes. (d) Surface porosity and (e) MD performance of the SDS10k-22 composite membranes prepared by swelling in C6 for varied durations.

exhibited salt rejections above 99.99%. That is, the MD performances of the three SDS composite membranes were very close to each other regardless of their various PDMS molecular weights. This should be attributed to the amount of water vapor passing through the membranes depended on the porosities of membranes rather than the pore size.

As the LEP value is inversely proportional to the surface pore size, changing the surface pore sizes of membranes by using SDS with different PDMS molecular weights may also influence the wetting resistance of membranes without tuning the WCAs. As shown in Fig. 6b, all three membranes exhibited high LEP values, which were increased with the decline of the PDMS molecular weight. The LEP values for SDS5k-24, SDS10k-22 and SDS25k-20 were 5.1, 4.4 and 3.7 bar, respectively. The WCAs of these three membranes were all 120° or so (Fig. S3), so the variation in LEPs should be attributed to that SDS with

lower PDMS molecular weights obtained smaller pore sizes. Such high LEP values indicated the composite membranes possessed good wetting resistance which could avoid pore wetting during long-term MD operations. Despite the molecular weight hardly influence the WCAs of membranes, the decrease in molecular weight indeed brings smaller pore sizes, and consequently better wetting resistance. In contrast, for commonly used microfiltration membranes, the increase of LEP value could only be achieved by increasing the WCAs [39].

3.4. Effect of swelling durations

Except for the effect of molecular weight, the effect of swelling durations on the MD performance was also studied. In addition to the overall porosity, the surface porosity of SDS10k-22 membranes also reached a constant value after swelling in C6 for 4 h at 25 °C (Fig. 6d), implying that the real equilibrium swelling condition was reached when the swelling duration was 4 h. In this case, it is expected that all pores are interconnected and no blind pores exist. Fig. 6e shows the permeate flux and salt rejection performance of the SDS10k-22 composite membrane as the function of the swelling duration. After swelling in C6 for only 1 min, the SDS10k-22 composite membrane exhibited a permeate flux of 10.3 kg m^{-2} h^{-1} and a 99.99% salt rejection. As the swelling duration was extended to 1 h, a slight increase of permeate flux to 13.2 kg m^{-2} h^{-1} was observed. However, with the swelling duration further increasing to 4 h, the permeate flux was increased to 17.8 kg m^{-2} h^{-1}. Further prolonging the swelling duration, the permeate flux and salt rejection did not show noticeable changes. The increase in permeate flux should be ascribed to the increment of the pore size and the porosity with extending swelling durations, as well as the interconnection of a small portion of blind pores (Fig. S7). Once the equilibrium swelling condition was reached, the porosities and pore sizes did not change obviously and no room for the permeate flux to grow.

3.5. Effect of thickness of the SDS coating layers

As microfiltration membranes used for MD usually displayed large pore sizes, poor hydrophobicity or large surface roughness, the effective hydrophobic separation layers were relatively thick and were usually tens of microns in thickness (Table S1). In contrast, the nanoporous SDS films prepared by selective swelling having pore sizes of only tens of nanometers could function as the effective MD layer with only several hundred nanometers in thickness. To elucidate the influence of the coating layer thickness on the MD performance, SDS10k-22 solutions with various concentrations were used to prepare composite membranes. Generally, a more dilute solution leads to a thinner coating layer, thus leading to lower mass transfer resistance. Fig. 7a–f show the cross-sectional SEM images of SDS10k-22 membranes with different dope solution concentrations ranging from 1 to 5 wt%. The coating layer with different film thicknesses all displayed uniform nanopores, which was distinguished from the macroporous PVDF substrates. As is presented in Fig. 7g, the thickness of the coating layers after swelling was increased to ~150, 470, 680, 980, 1400, and 2040 nm, respectively. When the dope solution concentration was less than 1 wt%, the coating layer was too thin that defects occurred easily, as-prepared composite membranes were easy to be wetted during MD.

As shown in Fig. 7h, the LEP value was also influenced by the thickness of the SDS layer to some extent. When the SDS solution concentration was 1 wt%, composite membranes displayed the smallest LEP

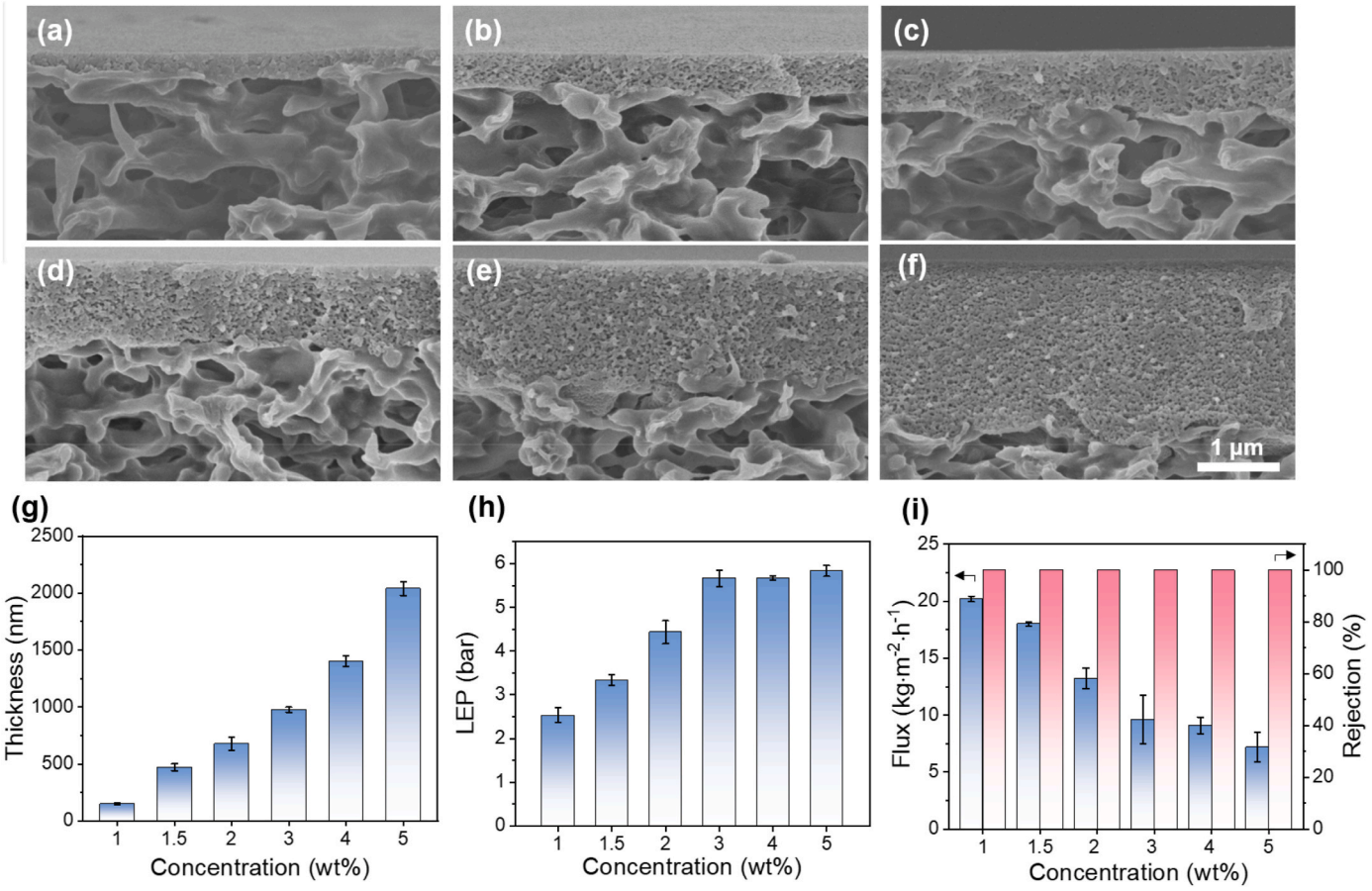

Fig. 7. (a–f) Cross-sectional SEM images of nanoporous SDS layers, all images have the same magnification as the scale bar given in (f). (g) Evolutions of the SDS layer thickness, (h) LEP values, and (i) MD performance with varied SDS solution concentrations. The selective swelling of SDS10k-22 composite membranes were performed in C6 for 1h.

value of 2.5 bar, which could also be comparative with other MD membranes [5]. With the increase of the SDS concentration, the LEP value was enhanced and reached a saturated value when the solution exceeded 3 wt%. When the film thickness exceeded 980 nm, the LEP values were close to 5.7 bar. Fig. 7i shows the effect of the SDS concentration on membrane performances. When the thickness was only ~150 nm, the SDS10k-22 composite membrane exhibited the highest permeate flux of 20.2 kg m^{-2} h^{-1} while the salt rejection still maintained 99.99%. As the solution concentration increased from 2 wt% to 3 wt%, the flux declined from 13.2 kg m^{-2} h^{-1} to 9.6 kg m^{-2} h^{-1}. This is because a thicker separation layer contributed more mass transfer resistance. In addition, when the SDS10k-22 concentration exceeded 3 wt%, the composite membranes showed only slightly decreased permeate flux. The permeate flux was still 7.2 kg m^{-2} h^{-1} when the solution concentration reached 5 wt%.

3.6. Evaluation of MD performances under different conditions

We have previously proved that the PDMS phase migrated to pore walls as well as the film surface after swelling, thus endowing the SDS membrane surface with permanent hydrophobicity. The long-term MD performance of the SDS10k-22 membranes swelling in C6 for 1 h is shown in Fig. 8a. During the MD evaluation for 156 h, the permeate flux of the SDS10k-22 membrane remained at around 14.2 kg m^{-2} h^{-1} and the rejection to NaCl was always greater than 99.99%. We also studied the effect of surfactants on the long-term performance of SDS10k-22 membranes. As shown in Fig. S8, the membranes still maintained almost unchanged flux and salt rejection after running MD at 50 °C for 156 h even in the presence of 0.05 mM sodium dodecyl sulfonic acid. Therefore, the SDS composite membranes prepared by selective swelling exhibited stable MD performance without any loss of salt rejection. This should be attributed to the outstanding wetting resistance (a high LEP value of 4.4 bar), smaller pore sizes and narrower pore size distribution compared to other MD membranes having pores in the range of microfiltration.

Furthermore, the permeate flux of SDS membranes could also be improved by adjusting other parameters. To better understand the effect of temperature on the permeate flux and verify the thermal stability of SDS composite membranes, the MD tests were conducted at different feed temperatures. As shown in Fig. 8b, the permeate flux of SDS membranes increased dramatically with the ever-increasing feed temperatures. At a low feed temperature of 30 °C, the permeate flux was only 4.0 kg m^{-2} h^{-1}. When the feed temperature was increased to 50 °C, the permeate flux was increased to 13.2 kg m^{-2} h^{-1}. It is interesting that the SDS10k-22 composite membrane could be well used at a high feed temperature of 80 °C, in which the permeate flux was as high as 32.8 kg m^{-2} h^{-1} with the rejection to NaCl maintained above 99.99%. The enhanced permeate flux was ascribed to the increased driving force caused by the higher temperature difference between the permeate and feed side so that more water vapor molecules passed through the SDS membrane pores. Therefore, higher flux could be achieved by minimizing the film thickness as possible and elevating the feed temperature of feed liquids without sacrificing the salt rejection performance (99.99%).

Therefore, SDS composite membranes with hydrophobic nanoporous layers with pore sizes in the ultrafiltration range prepared by selective swelling could be well used in MD while the membranes exhibited outstanding and stable performances. Compared to other MD membranes under the VMD condition in the literature (Fig. 9, detailed information was listed in Table S1), the SDS composite membranes in this work showed several advantages. First, all the SDS composite membranes exhibited a >99.99% rejection to NaCl and high LEP values larger than 2.5 bar, which are much higher than other membranes. Second, the flux of SDS composite membranes can be enhanced by adjusting the parameters, and the permeate flux could be as high as 32.8 kg m^{-2} h^{-1} at the feed temperature of 80 °C. More importantly, the effective layer of SDS composite membranes could reach as thin as hundreds of nanometers as a result of the small pore sizes (tens of nanometers) in the coating SDS layers. Considering the separation layers of most MD membranes were tens of micrometers in thickness, the SDS composite membranes with such thin coating layers consume much fewer materials and solvents.

4. Conclusions

In summary, we report a new type of composite membranes for membrane distillation with hydrophobic ultrafiltration membranes as the functional coating layer. The porous hydrophobic layer is prepared

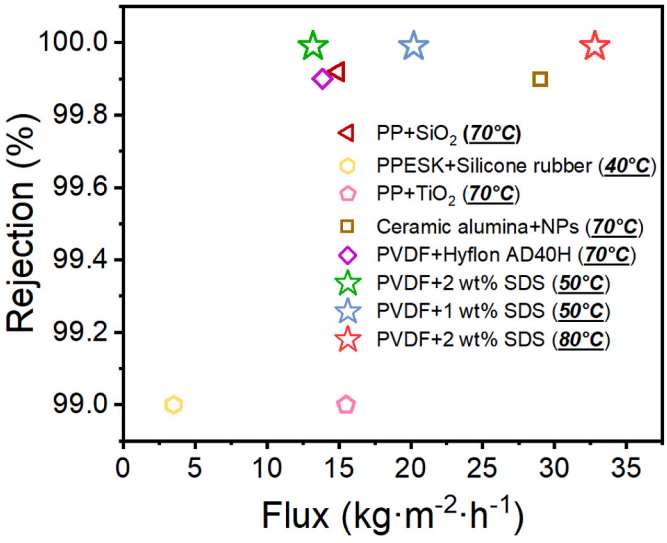

Fig. 9. Performance comparison of the SDS10k-22 composite membrane with other MD membranes [40–45].

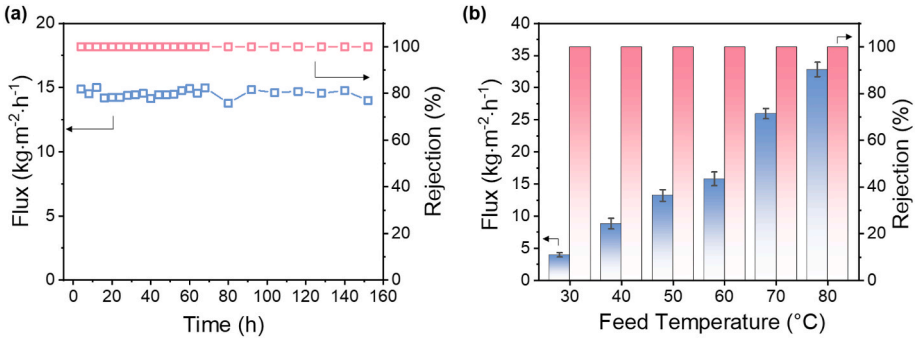

Fig. 8. (a) Long-term MD performance of the SDS10k-22 membrane swelling in C6 for 1 h, and (b) MD performance of the membrane at varied feed temperatures.

by a simple coating and selective swelling of SDS (polystyrene-*block*-polydimethylsiloxane-*block*-polystyrene) films at room temperature. The volume porosities and pore sizes of the swollen SDS films are strongly affected by the composition of SDS, swelling durations and the selective solvents. When the weight percentage of PDMS blocks is around 20%, the SDS films can reach high volume porosities of ~50% regardless of the molecular weight. Typically, the highest volume porosity of 50.2% is achieved with SDS10k-22 as the coating material and *n*-hexane as the swelling solvent. Besides, the pore sizes on film surface, and therefore the wetting resistance, increase dramatically with the molecular weight of PDMS while the porosities hardly changed. All SDS composite membranes show high LEP values above 2.5 bar although their WCAs are only ~120°. The LEP values can also be increased by increasing the film thickness when thinner than 1000 nm. The MD permeate flux is mainly affected by several factors including pore sizes, porosities and thickness of the nanoporous SDS layers, and the rejection to NaCl always exceeds 99.99%. Besides, the SDS composite membranes can tolerate high feed temperatures of 80 °C. In this condition, the permeate flux increases drastically to 32.8 kg $m^{-2}{\cdot}h^{-1}$ without sacrificing the rejection performance. Furthermore, the SDS composite membranes display excellent long-term stability. Therefore, this work demonstrates that hydrophobic SDS films with pore sizes in the ultrafiltration range prepared by selective swelling can be used as MD membranes, and thus-obtained membranes display excellent and long-standing MD performance.

CRediT authorship contribution statement

Zhuo Li: Investigation, Data curation, Writing – review & editing, Validation. **Shoutian Qiu:** Conceptualization, Investigation, Data curation, Writing – original draft, Writing – review & editing, Funding acquisition. **Xiang Ying:** Investigation, Methodology. **Fangli Zhang:** Investigation. **Xianli Xu:** Methodology. **Zhaoliang Cui:** Methodology, Validation. **Yong Wang:** Conceptualization, Writing – review & editing, Supervision, Funding acquisition.

Declaration of competing interest

The authors declare that they have no known competing financial interests or personal relationships that could have appeared to influence the work reported in this paper.

Data availability

Data will be made available on request.

Acknowledgements

Financial support from the National Natural Science Foundation of China (22108117, 21825803) is gratefully acknowledged.

Appendix A. Supplementary data

Supplementary data to this article can be found online at https://doi.org/10.1016/j.memsci.2023.121710.

References

[1] S. Santoro, A.H. Avci, A. Politano, E. Curcio, The advent of thermoplasmonic membrane distillation, Chem. Soc. Rev. 51 (2022) 6087–6125.
[2] H. Chamani, J. Woloszyn, T. Matsuura, D. Rana, C.Q. Lan, Pore wetting in membrane distillation: a comprehensive review, Prog. Mater. Sci. 122 (2021), 100843.
[3] L. Eykens, K. De Sitter, C. Dotremont, L. Pinoy, B. Van der Bruggen, Membrane synthesis for membrane distillation: a review, Sep. Purif. Technol. 182 (2017) 36–51.
[4] A. Abdel-Karim, S. Leaper, C. Skuse, G. Zaragoza, M. Gryta, P. Gorgojo, Membrane cleaning and pretreatments in membrane distillation – a review, Chem. Eng. J. 422 (2021), 129696.
[5] M. Qasim, I.U. Samad, N.A. Darwish, N. Hilal, Comprehensive review of membrane design and synthesis for membrane distillation, Desalination 518 (2021), 115168.
[6] A. Alkhudhiri, N. Hilal, Membrane distillation - principles, applications, configurations, design, and implementation, in: Emerging Technologies for Sustainable Desalination Handbook, 2018, pp. 55–106.
[7] M. Khayet, Membranes and theoretical modeling of membrane distillation: a review, Adv. Colloid Interface Sci. 164 (2011) 56–88.
[8] D. Curto, V. Franzitta, A. Guercio, A review of the water desalination technologies, Appl. Sci. 11 (2021) 670.
[9] J. Kujawa, E. Guillen-Burrieza, H.A. Arafat, M. Kurzawa, A. Wolan, W. Kujawski, Raw juice concentration by osmotic membrane distillation process with hydrophobic polymeric membranes, Food Bioprocess Technol. 8 (2015) 2146–2158.
[10] G. Lewandowicz, W. Białas, B. Marczewski, D. Szymanowska, Application of membrane distillation for ethanol recovery during fuel ethanol production, J. Membr. Sci. 375 (2011) 212–219.
[11] S. Fatima, B. Govardhan, S. Kalyani, S. Sridhar, Extraction of volatile organic compounds from water and wastewater by vacuum-driven membrane process: a comprehensive review, Chem. Eng. J. 434 (2022), 134664.
[12] H. Julian, N. Nurgirisia, G. Qiu, Y.P. Ting, I.G. Wenten, Membrane distillation for wastewater treatment: current trends, challenges and prospects of dense membrane distillation, J. Water Process Eng. 46 (2022), 102615.
[13] K.J. Lu, Y. Chen, T.S. Chung, Design of omniphobic interfaces for membrane distillation - a review, Water Res. 162 (2019) 64–77.
[14] G.D. Kang, Y.M. Cao, Application and modification of poly(vinylidene fluoride) (PVDF) membranes - a review, J. Membr. Sci. 463 (2014) 145–165.
[15] H. Kim, T. Yun, S. Hong, S. Lee, Experimental and theoretical investigation of a high performance PTFE membrane for vacuum-membrane distillation, J. Membr. Sci. 617 (2021), 118524.
[16] M. Gryta, The study of performance of polyethylene chlorinetrifluoroethylene membranes used for brine desalination by membrane distillation, Desalination 398 (2016) 52–63.
[17] L. Eykens, K. De Sitter, C. Dotremont, L. Pinoy, B. Van der Bruggen, Characterization and performance evaluation of commercially available hydrophobic membranes for direct contact membrane distillation, Desalination 392 (2016) 63–73.
[18] H. Susanto, Towards practical implementations of membrane distillation, Chem. Eng. Process 50 (2011) 139–150.
[19] W.A.F. Wae AbdulKadir, A.L. Ahmad, O.B. Seng, N.F. Che Lah, Biomimetic hydrophobic membrane: a review of anti-wetting properties as a potential factor in membrane development for membrane distillation (MD), J. Ind. Eng. Chem. 91 (2020) 15–36.
[20] A. Rastegarpanah, H.R. Mortaheb, Surface treatment of polyethersulfone membranes for applying in desalination by direct contact membrane distillation, Desalination 377 (2016) 99–107.
[21] J. Wang, H. He, M. Wang, Z. Xiao, Y. Chen, Y. Wang, J. Song, X.M. Li, Y. Zhang, T. He, 3-[[3-(Triethoxysilyl)-propyl] amino] propane-1-sulfonic acid zwitterion grafted polyvinylidene fluoride antifouling membranes for concentrating greywater in direct contact membrane distillation, Desalination 455 (2019) 71–78.
[22] C. Yang, M. Tian, Y. Xie, X.-M. Li, B. Zhao, T. He, J. Liu, Effective evaporation of CF4 plasma modified PVDF membranes in direct contact membrane distillation, J. Membr. Sci. 482 (2015) 25–32.
[23] H. Zhang, B. Li, D. Sun, X. Miao, Y. Gu, SiO2-PDMS-PVDF hollow fiber membrane with high flux for vacuum membrane distillation, Desalination 429 (2018) 33–43.
[24] L. Jiao, K. Yan, J. Wang, S. Lin, G. Li, F. Bi, L. Zhang, Low surface energy nanofibrous membrane for enhanced wetting resistance in membrane distillation process, Desalination 476 (2020), 114210.
[25] M.S. El-Bourawi, Z. Ding, R. Ma, M. Khayet, A framework for better understanding membrane distillation separation process, J. Membr. Sci. 285 (2006) 4–29.
[26] J. Pan, X. Xu, Z. Wang, S.P. Sun, Z. Cui, L. Gzara, I. Ahmed, O. Bamaga, M. Albeirutty, E. Drioli, Innovative hydrophobic/hydrophilic perfluoropolyether (PFPE)/polyvinylidene fluoride (PVDF) composite membrane for vacuum membrane distillation, Chin. J. Chem. Eng. 45 (2022) 248–257.
[27] L. Eykens, K. De Sitter, C. Dotremont, L. Pinoy, B. Van der Bruggen, How to optimize the membrane properties for membrane distillation: a review, Ind. Eng. Chem. Res. 55 (2016) 9333–9343.
[28] H. Nassrullah, O. Makanjuola, I. Janajreh, F.A. AlMarzooqi, R. Hashaikeh, Incorporation of nanosized LTL zeolites in dual-layered PVDF-HFP/cellulose membrane for enhanced membrane distillation performance, J. Membr. Sci. 611 (2020), 118298.
[29] M. Khayet, T. Matsuura, Preparation and characterization of polyvinylidene fluoride membranes for membrane distillation, Ind. Eng. Chem. Res. 40 (2001) 5710–5718.
[30] S. Zhao, C. Jiang, J. Fan, S. Hong, P. Mei, R. Yao, Y. Liu, S. Zhang, H. Li, H. Zhang, C. Sun, Z. Guo, P. Shao, Y. Zhu, J. Zhang, L. Guo, Y. Ma, J. Zhang, X. Feng, F. Wang, H. Wu, B. Wang, Hydrophilicity gradient in covalent organic frameworks for membrane distillation, Nat. Mater. 20 (2021) 1551–1558.
[31] X. Wei, B. Zhao, X.-M. Li, Z. Wang, B.-Q. He, T. He, B. Jiang, CF4 plasma surface modification of asymmetric hydrophilic polyethersulfone membranes for direct contact membrane distillation, J. Membr. Sci. 407–408 (2012) 164–175.
[32] S. Qiu, Z. Li, X. Ye, X. Ying, J. Zhou, Y. Wang, Selective swelling of polystyrene (PS)/poly(dimethylsiloxane) (PDMS) block copolymers in alkanes, Macromolecules 56 (2023) 215–225.

[33] D. Liu, J. Cao, M. Qiu, G. Zhang, Y. Hong, Enhanced properties of PVDF nanofibrous membrane with liquid-like coating for membrane distillation, Sep. Purif. Technol. 295 (2022), 121282.
[34] J. Sheng, M. Zhang, Y. Xu, J. Yu, B. Ding, Tailoring water-resistant and breathable performance of polyacrylonitrile nanofibrous membranes modified by polydimethylsiloxane, ACS Appl. Mater. Interfaces 8 (2016) 27218–27226.
[35] R.B. Saffarini, B. Mansoor, R. Thomas, H.A. Arafat, Effect of temperature-dependent microstructure evolution on pore wetting in PTFE membranes under membrane distillation conditions, J. Membr. Sci. 429 (2013) 282–294.
[36] Y. Wang, C. Zhang, J. Zhou, Y. Wang, Room-temperature swelling of block copolymers for nanoporous membranes with well-defined porosities, J. Membr. Sci. 608 (2020), 118186.
[37] J. Zhou, C. Zhang, C. Shen, Y. Wang, Synthesis of poly(2-dimethylaminoethyl methacrylate)-block-poly(styrene-alt-N-phenylmaleimide) and its thermo-tolerant nanoporous films prepared by selective swelling, Polymer 164 (2019) 126–133.
[38] J. Zhou, Y. Wang, Selective swelling of block copolymers: an upscalable greener process to ultrafiltration membranes? Macromolecules 53 (2020) 5–17.
[39] H.T. Nguyen, H.M. Bui, Y.-F. Wang, S.-J. You, Non-fluoroalkyl functionalized hydrophobic surface modifications used in membrane distillation for cheaper and more environmentally friendly applications: a mini-review, Sustain. Chem. Pharm. 28 (2022), 100714.
[40] W. Zhong, J. Hou, H.-C. Yang, V. Chen, Superhydrophobic membranes via facile bio-inspired mineralization for vacuum membrane distillation, J. Membr. Sci. 540 (2017) 98–107.
[41] M.A. Tooma, T.S. Najim, Q.F. Alsalhy, T. Marino, A. Criscuoli, L. Giorno, A. Figoli, Modification of polyvinyl chloride (PVC) membrane for vacuum membrane distillation (VMD) application, Desalination 373 (2015) 58–70.
[42] Z. Jin, D.L. Yang, S.H. Zhang, X.G. Jian, Hydrophobic modification of poly (phthalazinone ether sulfone ketone) hollow fiber membrane for vacuum membrane distillation, J. Membr. Sci. 310 (2008) 20–27.
[43] L. Zhang, Y. Feng, Y. Li, Y. Jiang, S. Wang, J. Xiang, J. Zhang, P. Cheng, N. Tang, Stable construction of superhydrophobic surface on polypropylene membrane via atomic layer deposition for high salt solution desalination, J. Membr. Sci. 647 (2022), 120289.
[44] C.Y. Huang, C.C. Ko, L.H. Chen, C.T. Huang, K.L. Tung, Y.C. Liao, A simple coating method to prepare superhydrophobic layers on ceramic alumina for vacuum membrane distillation, Sep. Purif. Technol. 198 (2018) 79–86.
[45] Z.L. Cui, Y.X. Zhang, X. Li, X.Z. Wang, E. Drioli, Z.H. Wang, S.F. Zhao, Optimization of novel composite membranes for water and mineral recovery by vacuum membrane distillation, Desalination 440 (2018) 39–47.